Corrosion potential of steel embedded in alkali-activated slag

Runci, Antonino; Serdar, Marijana

DOI: https://doi.org/10.5592/CO/PhDSym.2020.15

Corrosion potential of steel embedded in alkali-activated slag

Antonino Runci[1], Asst. Prof. **Marijana Serdar**[2]

[1]University of Zagreb, Faculty of Civil Engineering, Department of Materials, antonino.runci@grad.unizg.hr
[2]University of Zagreb, Faculty of Civil Engineering, Department of Materials, marijana.serdar@grad.unizg.hr

Abstract

Alkali-Activated Materials (AAMs) are a group of free clinker binders that are based on aluminosilicate powder and an alkali activator. AAMs have shown high performance in many areas and have attracted great interest because of their lower environmental impact compared to ordinary Portland cement. The aim of this paper is to offer a first assessment on the safety of application of AAMs in marine environments, or where de-icing salts are used. The paper focuses on the alkali-activated ground-granulated blast furnace slag in combination with other by-products originating from Southeast Europe. The setup used to evaluate the corrosion behaviour consists of structural steel plates covered with a layer of mortar, and with tap water or a simulated seawater solution. The corrosion behaviour of structural steel plates was monitored by means of the Open Circuit Potential (OCP).

Key words: alkali-activated material, slag, durability, corrosion potential, steel corrosion

Korozijski potencijal čelika ugrađenog u alkalno-aktiviranu zguru

Sažetak

Alkalno aktivirani materijali (AAM) su bezcementna veziva na bazi alumino-silikatnog praha i alkalnog aktivatora. Zbog smanjenog utjecaja na okoliš i visokih uporabnih svojstava, u usporedbi s običnim portlandskim cementom, ovakvi materijali privlače pozornost znanstvenika i industrije. Cilj ovog rada je pružiti prvu procjenu sigurne primjene AAM-a u morskom okolišu ili tamo gdje se koriste soli za odmrzavanje. U radu je korištena alkalno aktivirana granulirana zgura visokih peći u kombinaciji s ostalim industrijskim nusproizvodima s područja jugoistočne Europe u svrhu praćenja korozije. Korištena metoda sastoji se od konstrukcijskih čeličnih ploča prekrivenih slojem morta te slojem vode, odnosno slojem simulirane otopine morske vode. Korozijsko ponašanje konstrukcijskih čeličnih ploča praćeno je potencijalom otvorenog kruga (engl. Open Circuit Potential - OCP).

Ključne riječi: alkalno aktivirani materijal, zgura, trajnost, korozijski potencijal, korozija čelika

1 Introduction

Alkali-activated materials (AAMs) are a group of clinker-free binders that have been developed over the last century. These materials have recently attracted considerable interest due to rapid growth of new urban areas, particularly in developing countries, and the growing demand for materials with low environmental impact. Portland cement production currently account for 8% of global anthropological CO_2 emissions and the growing demand for building materials could increase production from 3.6 billion tons (Gt) to 3.7–5.5 Gt per year [1]. This aspect contrasts with the global trend of decarbonisation, and the commitments made under Paris agreement in 2015.

AAMs represent a valid alternative to Portland cement, since only small amounts of CO_2 are emitted due to the production of alkali activator, which generally accounts for less than 10% of the total binder content. The alkali activators used are usually based on Na or K and can be a liquid solution that is added to precursors together with water during the mixing process, or a solid salt in the one-part system that is premixed with dry precursors [2, 3]. In addition, AAMs are based on aluminosilicate powder that is usually a by-product of other industrial activities such as steel production and/or coal-fired power plants, which reduces the amount of raw material needed for clinker production [3]. Habert et al. [4] have already shown that this type of system is highly efficient in reducing CO2 emissions compared to OPC, despite some problems related to other outstanding environmental impact categories.

Chemical variability of precursors is the greatest limitation to standardization, and thus to the application of these binders. AAMs can generally be divided into two different categories based on composition of the final phase [3]: (I) low Ca systems - based on activation of a low Ca precursor, such as fly ash or metakaolin, the main reaction product being a three-dimensional gel of the alkali-aluminosilicate hydrate (N- A-S-H) type; and (II) high Ca systems - based on activation of a high Ca precursor, such as blast furnace slag, the main reaction product being a gel of the calcium-aluminosilicate-hydrate (C-A-S-H) type.

The work of RILEM TC 247-DTA [5] has recently shown that the existing standards specified for OPC are also applicable to AAMs. This information is not sufficient to justify the use of AAMs in corrosive environments such as marine environments or environments in which de-icing salts are used, because chloride penetration and subsequent steel corrosion in reinforced concrete is the main cause of early corrosion of steel reinforcement in all countries across the world [6]. Babaee and Castel [7] have tested main possible combinations of AAMs with chloride ingress and embedded steel resistance. The results have shown that high Ca systems have a higher resistance to chloride penetration than low Ca systems, as confirmed by RILEM TC

247-DTA [8]. The reasons for the difference in behaviour are not entirely clear, but the basic influence of the gel phases and the hydration product structure has been the most widely accepted theory so far.
In this short paper, the alkali-activated blast furnace slag was tested in combination with other by-products originating from Southeast Europe in the chloride-containing environment. This paper focuses on the corrosion potential (E_{corr}) as the main index of corrosion initiation.

2 Mix design and method

A commercial ground granulated blast furnace slag from Lafarge Holcim was used as the main component of the mix, in combination with other by-products: fly ash class F from Elektroprivreda, silica fume from R-D Silicon D.O.O. (Bosnia & Herzegovina), and iron-silicate fines from Aurubis (Bulgaria). Chemical composition of by-products used in the formulations is shown in Table 1.

Table 1. Chemical composition of by-products in wt.%

	CaO	SiO_2	Al_2O_3	Fe_2O_3	Na_2O	K_2O	MgO	TiO_2	MnO	SO_3	P_2O_5
Blast furnace slag	33.46	41.59	12.84	0.73	1.39	0.57	5.97	1.73	0.08	1.65	0.01
Fly ash	13.04	51.1	20.58	7.42	0.89	1.99	2.15	0.53	0.04	1.72	0.54
Silica fume	3.06	92.02	1.68	0.45	0.21	1.11	0.77	0.04	0.03	0.27	0.36
Iron-silicate fine	2.7	27.5	3.5	66.5	0.4	0.9	0.7	0	0	0.7	0

In the present study, precursors were activated with sodium silicate Geosil 34417 from Woellner with Ms = 1.68 and NaOH 17.8 M solution or potassium silicate Geosil 14515 from Woellner with Ms = 1.5. The aggregate was local dolomite sand with the 0-4 mm grain size. The precursors/aggregate ratio used was 0.3. The mix design is summarized in Table 2.

Table 2. Mortar mix design assessed in this study (in wt%)

Label	Blast furnace slag	Fly ash	Iron-silicate fine	Silica fume	NaOH	Waterglass		Water
						KSi	NaSi	
AAS	67.7	0	0	0	5.4	0	4.2	22.7
AASFA	56.8	18.9	0	0	7.2	0	10.4	6.6
AAIS	13.8	0	55.5	0	0	13.8	0	16.6
AASF	53.2	0	0	13.8	9.4	0	15	13.1

The samples were mixed for 9 minutes in total. The dry components were homogenized for 1 minute, the mixtures were mixed for 6 minutes with the addition of the liquid solution, and the mixing was interrupted for 1 minute and was then resumed for another minute.

The steel corrosion over time was monitored by the open circuit potential (OCP). The measurements were performed with an unconventional three-electrode cell (Figure 1) following the example of Šoić et al. [9] using a PAR VMP2 potentiostat/galvanostat. The samples were prepared with a mild steel plate as working electrode simulating reinforcement inside mortar, with a surface area of 4.415 cm^2 exposed to mortar. Carbon steel plates were polished until an even metallic surface was obtained. A polymer cylinder with silicone was glued onto the steel plate. This cylinder was used as a mould in which the mortar was poured to 2 cm in thickness. After 7 days of curing in sealed conditions, the electrolyte solution was placed in each cell (3 per mixture) on top of mortar; tap water or 0.62 M NaCl solution was used as electrolyte to simulate sea water. A saturated calomel electrode (SCE) was positioned in the solution to serve as reference electrode (Figure 1). The samples were covered with plastic foil to prevent electrolyte evaporation in the time between measurements. The open-circuit potential (OCP) measurement was performed regularly for 15 minutes.

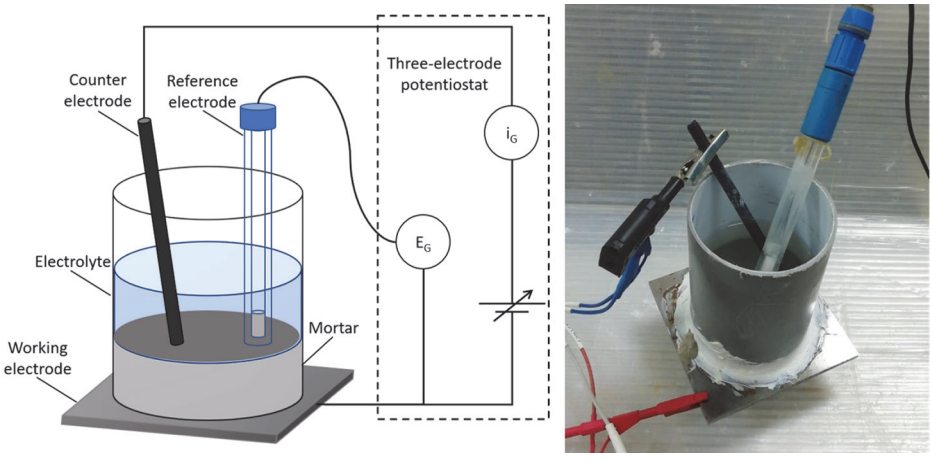

Figure 1. Three-electrode cell set-up

Corrosion potential (E_{corr}) is the most common corrosion index, but it is only a qualitative parameter. The tendency of metal to corrode can be assessed based on corrosion potential, i.e. its change over time. If the OCP is stable or tends towards more positive values, it can be assumed that the passive film around metal is stable in this medium. If the OCP tends towards more negative values, it can be assumed

that the passive film on metal is unstable and that local corrosion will occur or has already occurred. Table 3 shows limit values of corrosion potential and polarization resistance (R_p) used for OPC compared to evolution of steel passive film.

Table 3. Index values of corrosion potential (E_{corr}) and polarization resistivity (R_p) for OPC [10]

Risk of corrosion	E_{corr} [mV]	R_p [kΩ·cm²]
Passive condition (> 90 % probability of having no corrosion)	$E_{corr} > -200$	$R_p > 250$
Very low-to-moderate corrosion rate	$-200 < E_{corr} < -300$	$25 < R_p < 250$
High corrosion rate (> 90 % probability of having active corrosion)	$E_{corr} < -300$	$R_p < 25$

3 Results and discussion

Potential development in reference and corrosion environments during the 220-day curing time is shown for four mixes in Figure 2.
In all samples except AASF the value of E_{corr} increased during the first 50 days and stayed stable in reference samples exposed to water. In simulated seawater, steel E_{corr} showed a stable trend in AAS until 200 days, when the E_{corr} value started to decrease, probably due to initiation of corrosion. AASFA and AAIS showed a progressive reduction of the potential up to 150 days. after that, the potential values were stable around -600 mV. In contrast, AASF showed a strong reduction of E_{corr} already prior to 50 days of exposure.

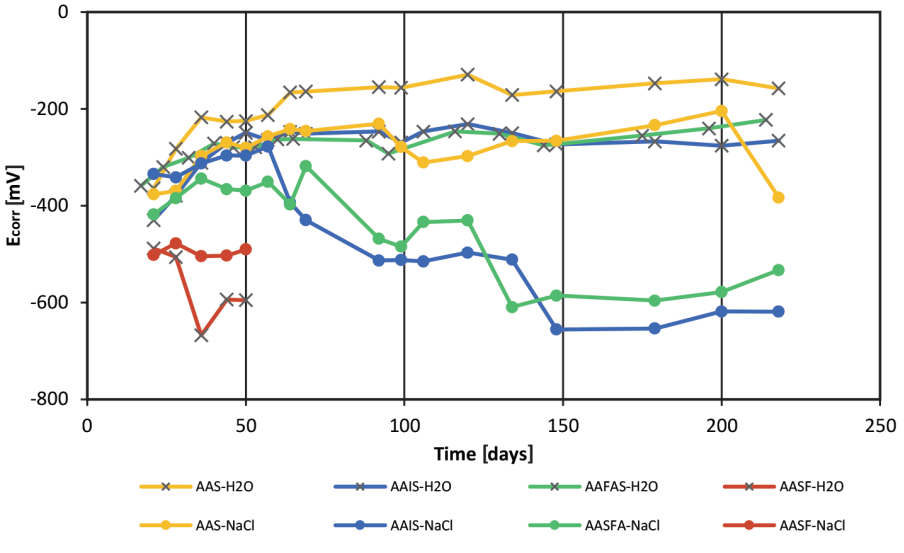

Figure 2. Corrosion Potential (E_{corr}) of mortar in reference water (x) and simulated seawater (•)

The AAMs showed lower potential values than OPC in both corrosive and reference environments (Table 3). This lower value of the corrosion potential could be attributed to oxygen consumption by sulphides in pore solution [7, 11] and Mackinawite precipitates on the steel surface [12]. In the first 50 days the increase of E_{corr} is probably associated with a delay in passive film formation, as already shown by [12]: between 50 and 60 days all mixtures except AASF maintained the passive film formation trend.

The early corrosion of AASFA and AAIS with respect to AAS is probably associated with the porosity effect and the chloride binding capacity (P_{cb}). As has already been shown, low Ca systems have higher porosity and permeability compared to high Ca systems [13, 14]. In addition, chloride ingress is partly hindered by higher binding capacity of high Ca systems due to chloride uptake by hydrotalcite and physical adsorption on C-A-S-H gel and possible precipitation of Friedel's Salts [15, 16]. Due to higher surface of N-A-S-H gel on which chloride is physically adsorbed, the P_{cb} in N-A-S-H is higher than in C-A-S-H. When blast furnace slag is replaced with fly ash, the C-A-S-H/N-A-S-H ratio decreases and the P_{cb} increases, resulting in pH decrease of the pore solution [7, 11]. These can justify faster reduction of corrosion potential for AASFA and AAIS.

In the case of AASF samples, it has been demonstrated that the filler effect of silica fume increases corrosion protection [17]. However, severe cracking on sample surface and detachment of mortar samples from the mould was observed in the case of AASF mix. This severe crack formation can be attributed to drying shrinkage. Due to this crack formation, sea water was in direct contact with structural steel, which prevented formation of passive film. It can therefore be concluded that observed values of potential were very low already after few days of exposure in the case of steel in AASF mix.

4 Conclusion and future prospective

Steel corrosion was monitored for up to 220 days of exposure to a simulated sea water solution. In this paper, steel corrosion is analysed through corrosion potential (E_{corr}). The corrosion potential observed in AAMs was lower compared to that usually registered in OPC. Nevertheless, it pointed to protection of steel surface by passive film formation. Deviations of electrochemical data from the OPC standard have already been established [7, 12], but standardized limits for AAMs still need to be developed. In addition, chemical compositions of precursors represent the greatest limitation to the safe use of AAMs. AAMs have a broad chemical and mineralogical composition. Blast furnace slag showed a high specific resistance to chloride, but systems mixed with fly ash, silica fume and iron-silica fines exhibit a higher corrosion risk. In particular, the lower stability of the AASFA passive layer may be related

to pore structure development: A lower pore refinement than in pure slag systems can influence the resistance [18], but the N-A-S-H influence on the chloride binding capacity is still to be fully understood. AAIS and AASF require further investigation at the compound design stage before moving on to the corrosion study.
The importance of mix design is underlined in the present study. Future research could involve analysis of corrosion rate and electrochemical impedance spectroscopy spectra, with the focus on correlation between electrochemical properties and microstructure of AAMs to validate the influence of porosity and mineralogical evolution on corrosion resistance. Furthermore, the influence of binder matrix and binding capacity on chloride penetration needs to be investigated to explain the difference between different AAMs. Additionally, a critical chloride content needs to be determined to evaluate the influence of compound design on corrosion resistance.

Acknowledgment

Research presented in this paper was performed within the DuRSAAM project, which has received funding from the European Union's Horizon 2020 research and innovation programme under the grant agreement No 813596. The research is also supported by the project "Alternative Binders for Concrete: understanding microstructure to predict durability, ABC", funded by the Croatian Science Foundation under No. UIP-05-2017-4767.

References

[1] Provis, J.: Green concrete or red herring? - Future of alkali-activated materials, Advances in Applied Ceramics, vol. 113, no. 8, pp. 472–477, 2014.

[2] Luukkonen, T.,Abdollahnejad, Z., Yliniemi, J., Kinnunen, P., Illikainen, M.: One-part alkali-activated materials: A review, Cement and Concrete Research, vol. 103, no. September 2017, pp. 21–34, 2018.

[3] Provis, J., van Deventer, J. S. J.: Alkali Activated Materials: State-of-the-Art Report, RILEM TC 224-AAM, vol. 13. 2014.

[4] Habert, g., D'Espinose De Lacaillerie, J. B., Roussel, N.: An environmental evaluation of geopolymer based concrete production: Reviewing current research trends, Journal of Cleaner Production, vol. 19, no. 11, pp. 1229–1238, 2011.

[5] Provis, J. et al.: RILEM TC 247-DTA round robin test: mix design and reproducibility of compressive strength of alkali-activated concretes, Materials and Structures, vol. 52, no. 5, pp. 1–13, 2019.

[6] Angst, U.: Challenges and opportunities in corrosion of steel in concrete, Materials and Structures/Materiaux et Constructions, vol. 51, no. 1, pp. 1–20, 2018.

[7] Babaee, M., Castel, A.: Chloride diffusivity, chloride threshold, and corrosion initiation in reinforced alkali-activated mortars: Role of calcium, alkali, and silicate content, Cement and Concrete Research, vol. 111, no. May, pp. 56–71, 2018.

[8] Gluth, G. J. G. et al.: RILEM TC 247-DTA round robin test : carbonation and chloride penetration testing of alkali-activated concretes, Materials and Structures, vol. 3, 2020.

[9] Šoić, I., Martinez, S., Lipošćak, I., Mikšić, B.: Development of method for assessing efficiency of organic corrosion inhibitors in concrete reinforcement, Gradjevinar, vol. 70, no. 5, pp. 369–375, 2018.

[10] American society for testing and materials, "ASTM C 876/09 - Standard Test Method for Half-Cell Potentials of Uncoated Reinforcing Steel in concrete.," Annual Book for ASTM Standards, American Society for Testing and Materials., vol. 91, no. Reapproved 1999, pp. 1–6, 2009.

[11] Ma, Q., Nanukuttan, S. V., Basheer, P. A. M., Bai, Y., Yang, C.: Chloride transport and the resulting corrosion of steel bars in alkali activated slag concretes, Materials and Structures/Materiaux et Constructions, vol. 49, no. 9, pp. 3663–3677, 2016.

[12] Mundra, S., Bernal, S. A., Criado, M., Hlavá, P., Ebell, G., Reinemann, S., Gregor, G. J. G., Provis, J.: Steel corrosion in reinforced alkali activated materials, RILEM Technical Letters 2: 33-39, 2017.

[13] Osio-Norgaard, J., Gevaudan, J. P., Srubar, W. V.: a review of chloride transport in alkali-activated cement paste, mortar, and concrete, Construction and Building Materials, vol. 186, pp. 191–206, 2018.

[14] Van Deventer, J. S. J., et al.: Microstructure and durability of alkali-activated materials as key parameters for standardization, Journal of Sustainable Cement-Based Materials, vol. 4, no. 2, pp. 120–134, 2015.

[15] Zhang, J., Shi, C., Zhang, Z.: Chloride binding of alkali-activated slag/fly ash cements, Construction and Building Materials, vol. 226, pp. 21–31, 2019.

[16] Ke, X., Bernal, S. A., Provis, J.: Uptake of chloride and carbonate by Mg-Al and Ca-Al layered double hydroxides in simulated pore solutions of alkali-activated slag cement, Cement and Concrete Research, vol. 100, no. October 2016, pp. 1–13, 2017.

[17] Rostami, M., Behfarnia, K.: The effect of silica fume on durability of alkali activated slag concrete, Construction and Building Materials, vol. 134, pp. 262–268, 2017.

[18] Ma, Y., Wang, G., Ye, G., Hu, J.: A comparative study on the pore structure of alkali-activated fly ash evaluated by mercury intrusion porosimetry, N2 adsorption and image analysis, Journal of Materials Science, vol. 53, no. 8, pp. 5958–5972, 2018.